J. Plasma Physics (2006), *vol.* 72, *part* 6, *pp.* 1081–1086. © 2006 Cambridge University Press
doi:10.1017/S002237780600568X Printed in the United Kingdom

Meshless structural analyses of complex shape models using implicit surface representations

KYOKO HASEGAWA[1],
SUSUMU NAKATA[2] and SATOSHI TANAKA[2]

[1]Centre for Promotion of the COE, Ritsumeikan University, Noji Higashi 1-1-1 Kusatsu, 525-8577 Shiga-ken, Japan

[2]College of Information Science and Engineering, Ritsumeikan University, Noji Higashi 1-1-1 Kusatsu, 525-8577 Shiga-ken, Japan

(Received 15 August 2005 and accepted 24 May 2006)

Abstract. In this paper, we present a scheme for analyzing structures which have complex shape models. The targets of the structural analysis usually consist of a combination of simple shape models generated using modeling tools such as CAD systems. On the other hand, in the field of computer graphics, there have been proposed a number of techniques that make it possible to create complex shape models from point clouds obtained by three-dimensional (3D) range scanners. One suitable representation for the reconstructed shape is an implicit surface model. One typical advantage of the implicit representation is fast inside/outside distinction. For the analysis of a structure represented as an implicit surface model, we use the Element-Free Galerkin Method (EFGM), which is suitable for the analysis of a structure with an implicit surface representation. For the analysis with the EFGM, internal nodes spread in the object are required and the nodes can be generated easily using the property of fast inside/outside distinction. We also note that the EFGM does not require any information about connectivity between adjoining nodes inside the model. We also present some numerical results of 3D stress problems.

1. Introduction

The Finite-Element Method (FEM) is one of the most popular techniques for structural analysis and has been widely used in various fields of engineering. Another important technique, the meshless method (or the Element-Free Galerkin Method (EFGM)), was proposed by Belytschko et al. in 1994 [1]; see also [2–4]. The principal advantage of this method is the omission of the meshing or remeshing process that often constitutes a bottleneck in FEM approaches for the analysis of three-dimensional (3D) objects. On the other hand, a number of methods have been developed for the generation of complex 3D geometric models from point data sets given by 3D range scanners [5–7]. The methods enable the objects to be reconstructed as implicit functions that interpolate the given data sets.

In this paper, we propose a method for structural analysis of 3D complex objects which have implicit surface representations. For the structural analysis we employ the meshless approach, which is suitable for analyzing such objects.

https://doi.org/10.1017/S002237780600568X Published online by Cambridge University Press

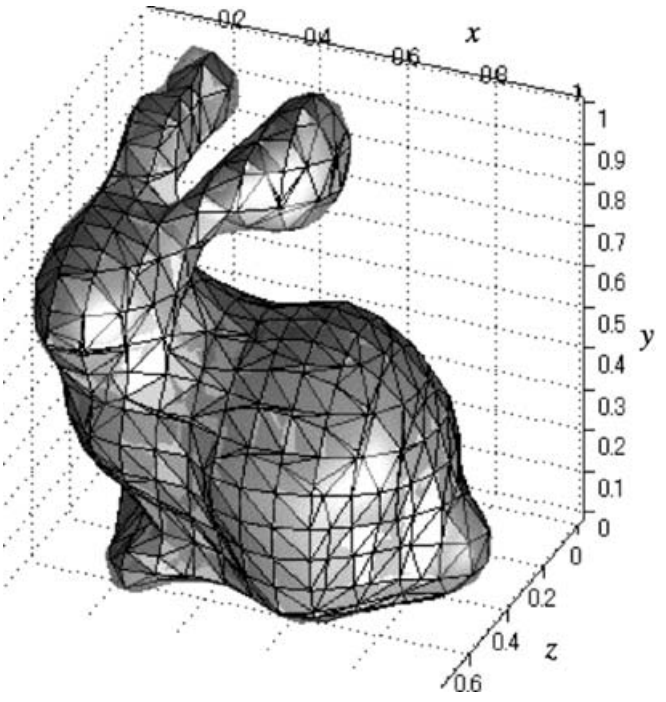


Figure 1. Target for elastic analysis and generated mesh on the surface (Stanford 3D Scanning Repository).

2. Modeling of 3D objects and node generation

An implicit surface is defined as a set of points satisfying $f(\mathbf{x}) = 0$ ($\mathbf{x} \in \mathbb{R}^3$) and we assume that the region $f(\boldsymbol{x}) > 0$ represents inside the surface. The purpose here is to create a function $f : \mathbb{R}^3 \to \mathbb{R}$ such that the implicit surface $f(\boldsymbol{x}) = 0$ interpolates or approximates the given point set. One well-known approach for the creation of the implicit function is the RBF (Radial Basis Functions) based method proposed by Turk and O'Brien [7], and we use this method for surface reconstructions throughout this paper. There is also a well-known approach proposed by Ohtake et al. [5] that is based on the idea of the partition of unity and it allows implicit functions to be created from a large number of input points. Note that the procedure we propose in this paper does not depend on the implicit surface reconstruction methods. We show an example of the object created by the Turk and O'Brien's method, in Fig. 1.

The next step is the generation of nodes distributed inside the surface required for the meshless analysis. The nodes can be generated using the fact that any point inside the surface satisfies $f(\boldsymbol{x}) > 0$. We also note that no connectivity information of the nodes inside the surface is required for the meshless analysis. An example of the nodes is shown in Fig. 2.

3. Meshless approach for 3D elasticity problems

In this section, we show the method of discretization of 3D elasticity problems using the EFGM approach [1, 2].

https://doi.org/10.1017/S002237780600568X Published online by Cambridge University Press

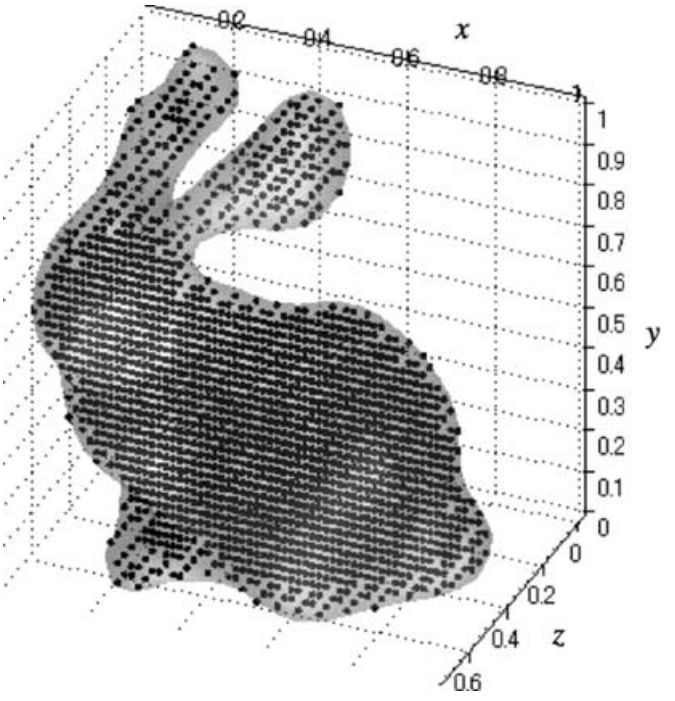


Figure 2. Nodes created inside the object.

3.1. 3D elasticity problems

In this section, we consider a 3D elasticity problem of an object represented as an implicit surface. We assume here that nodes inside the object are given. We employ the EFGM to solve the problem,

The elasticity problem is expressed using displacement of the object $\mathbf{p}(\boldsymbol{x}) = (u(\boldsymbol{x}), v(\boldsymbol{x}), w(\boldsymbol{x}))^{\mathrm{T}}$, strain $\varepsilon = (\varepsilon_x, \varepsilon_y, \varepsilon_z, \gamma_{xy}, \gamma_{yz}, \gamma_{zx})$ and stress $\sigma = (\sigma_x, \sigma_y, \sigma_z, \sigma_{xy}, \sigma_{yz}, \sigma_{zx})$ as

$$\begin{cases} \dfrac{\partial \sigma_x(\boldsymbol{x})}{\partial x} + \dfrac{\partial \sigma_{xy}(\boldsymbol{x})}{\partial y} + \dfrac{\partial \sigma_{zx}(\boldsymbol{x})}{\partial z} = 0, \\ \dfrac{\partial \sigma_{xy}(\boldsymbol{x})}{\partial x} + \dfrac{\partial \sigma_y(\boldsymbol{x})}{\partial y} + \dfrac{\partial \sigma_{yz}(\boldsymbol{x})}{\partial z} = 0, \\ \dfrac{\partial \sigma_{zx}(\boldsymbol{x})}{\partial x} + \dfrac{\partial \sigma_{yz}(\boldsymbol{x})}{\partial y} + \dfrac{\partial \sigma_z(\boldsymbol{x})}{\partial z} = 0, \end{cases} \begin{cases} \varepsilon_x = \dfrac{\partial u}{\partial x}, \\ \varepsilon_y = \dfrac{\partial v}{\partial y}, \\ \varepsilon_z = \dfrac{\partial w}{\partial z}, \end{cases} \begin{cases} \gamma_{xy} = \dfrac{\partial v}{\partial x} + \dfrac{\partial u}{\partial y}, \\ \gamma_{yz} = \dfrac{\partial w}{\partial y} + \dfrac{\partial v}{\partial z}, \\ \gamma_{zx} = \dfrac{\partial u}{\partial z} + \dfrac{\partial w}{\partial x}, \end{cases} \tag{3.1}$$

$$\boldsymbol{\sigma} = D\boldsymbol{\varepsilon}, \tag{3.2}$$

where D denotes a stress–strain matrix. We denote the load condition and the constraint condition of (3.1) as $\bar{\boldsymbol{q}} = (\bar{q}_x, \bar{q}_y, \bar{q}_z)^{\mathrm{T}}$ and $\bar{\boldsymbol{p}} = (\bar{u}, \bar{v}, \bar{w})^{\mathrm{T}}$, respectively.

3.2. Discretization by the EFGM

The discrete equation corresponding to (3.1) and (3.2) is obtained using the shape functions $\phi_i(\mathbf{x})$ that are the bases of MLS (Moving Least Squares) interpolation [1]. The bases are defined at all nodes of the object. The following discrete equations

https://doi.org/10.1017/S002237780600568X Published online by Cambridge University Press

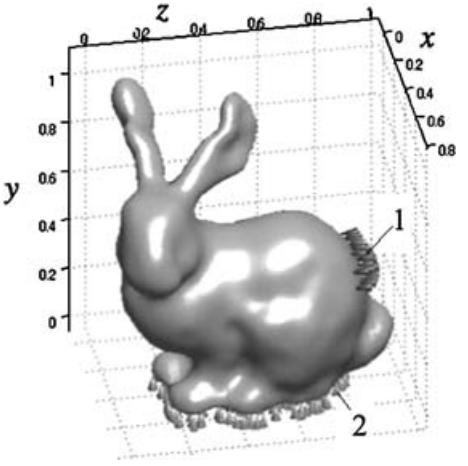


Figure 3. Boundary conditions. (arrow 1: load condition, arrow 2: constraint condition.)

are accordingly obtained:

$$u(\boldsymbol{x}) = \sum_{i=1}^{N} u_i \phi_i(\boldsymbol{x}), \quad v(\boldsymbol{x}) = \sum_{i=1}^{N} v_i \phi_i(\boldsymbol{x}), \quad w(\boldsymbol{x}) = \sum_{i=1}^{N} w_i \phi_i(\boldsymbol{x}), \tag{3.3}$$

$$\lambda(\boldsymbol{S}) = \sum_{k=1}^{M} \lambda_k N_k(\boldsymbol{S}), \tag{3.4}$$

where $(u_i, v_i, w_i)^{\mathrm{T}}$ is the displacement of each node, λ_k is a Lagrange multiplier and $N_k(\boldsymbol{S})$ is the shape function defined on the surface, see [1, 4] for more details. Hence, we obtain the following linear systems:

$$M\boldsymbol{u} - D\boldsymbol{\lambda} = \boldsymbol{f}, \tag{3.5}$$

$$-D^{\mathrm{T}}\boldsymbol{u} = -\boldsymbol{g}. \tag{3.6}$$

Here M and D are matrices evaluated using the shape function $\phi_i(\mathbf{x})$ and $N_k(\boldsymbol{S})$, respectively, and $\boldsymbol{u}$, λ, $\boldsymbol{f}$ and $\boldsymbol{g}$ are the displacement, the Lagrange multiplier, the load condition and the constraint condition, respectively.

By solving (3.5) and (3.6), the displacement $\mathbf{p}(\mathbf{x})$ can be obtained.

4. Numerical examples

In this section, we present numerical results of a 3D elasticity problem of the object shown in Fig. 1 (Stanford 3D Scanning Repository). This figure also shows the mesh on the surface used for the numerical integration to make the matrix D. The mesh can be obtained by polygonizing the implicit surface [8].

The load and the constraint conditions which we assumed are shown in Fig. 3. As shown in this figure, the load condition is defined around the back and the constraint condition is defined at the bottom. We show the result of the von Mises stress obtained under the above condition in Fig. 4. The von Mises stress is defined

https://doi.org/10.1017/S002237780600568X Published online by Cambridge University Press

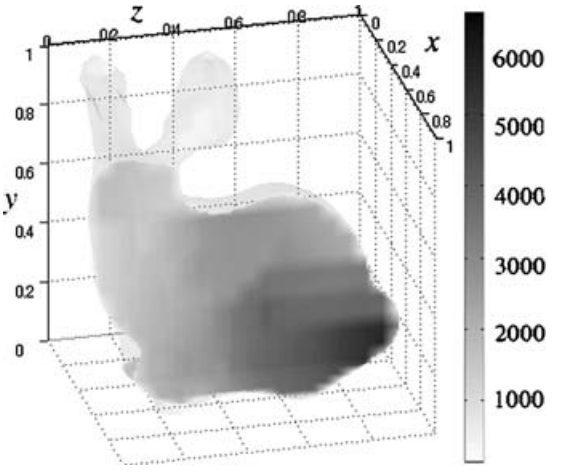


Figure 4. Numerical result: von Mises stress.

as

$$\bar{\sigma} = \sqrt{\{(\sigma_x - \sigma_y)^2 + (\sigma_y - \sigma_z)^2 + (\sigma_z - \sigma_x)^2 + 6(\sigma_{xy}^2 + \sigma_{yz}^2 + \sigma_{zx}^2)\}/2}, \qquad (4.1)$$

where the number of the nodes inside the object is 10 694, the number of the nodes on the surface is 143, shear elastic modulus is 7.52×10^{10} and Poisson's ratio is 0.33. In this figure, a *black part* indicates the maximum value of $\bar{\sigma}$. From the result, we see that a reliable result could be obtained.

5. Conclusion

In the present work an approach for the structural analysis of objects represented as implicit surfaces has been presented. We have shown that the analysis by the meshless approach is suitable for objects represented as implicit surface models. The analysis has been performed by the following process.

(1) Represent the shape of the object as an implicit surface model.
(2) Create nodes inside the object.
(3) Polygonize the surface.
(4) Discretize and solve the 3D elasticity problem using EFGM and visualize it.

References

[1] Belytschko, T., Lu, Y. Y. and Gu, L. 1994 Element-free Galerkin methods. *Int. J. Numer. Methods Eng.* **37**, 229–256.

[2] Dolbow, J. and Belytschko, T. 1999 Numerical integration of the Galerkin weak form in meshfree methods. *Comput. Mech.* **23**, 219–230.

[3] Nagashima, T. 1999 Node-by-node meshless approach and its applications to structural analyses. *Int. J. Numer. Methods Eng.* **46**, 341–385.

[4] Rahman, S. and Rao, B. N. 2001 An element-free Galerkin method for probabilistic mechanics and reliability. *Int. J. Solids Struct.* **38**, 9313–9330.

[5] Ohtake, Y., Belyaev, A., Alexa, M., Turk, G. and Seidel, H.-P. 2003 Multi-level partition of unity implicits. *ACM Trans. Graphics* **22**, 463–470.

https://doi.org/10.1017/S002237780600568X Published online by Cambridge University Press

[6] Savchenko, V. V., Pasko, A. A., Okunev, O. G. and Kunii, T. L. 1995 Function representation of solids reconstructed from scattered surface points and contours. *Comput. Graphics Forum* **14**, 181–188.

[7] Turk, G. and O'Brien, J. F. 2002 Modeling with implicit surfaces that interpolate. *Comput. Graphics Forum* **14**, 855–873.

[8] Bloomenthal, J. 1998 Polygonization of implicit surface. *Comput. Aided Geom. Design* **5**, 341–355.

https://doi.org/10.1017/S002237780600568X Published online by Cambridge University Press